Comparison of the Corrosion Protection of Mild Steel by Polypyrrole–Phosphate and Polypyrrole–Tungstenate Coatings

M. G. Hosseini,[1] M. Sabouri,[2] T. Shahrabi[2]

[1]*Electrochemistry Research Laboratory, Department of Physical Chemistry, Chemistry Faculty, University of Tabriz, Iran*
[2]*Department of Materials Science, Faculty of Engineering, Tarbiat Modarres University, Tehran, Iran*

Received 18 March 2007; accepted 15 May 2008
DOI 10.1002/app.28796
Published online 26 August 2008 in Wiley InterScience (www.interscience.wiley.com).

ABSTRACT: The electrodeposition of polypyrrole–phosphate (PPy–P) and polypyrrole–tungstenate (PPy–W) on mild steel (MS) were achieved in an oxalic acid medium with cyclic voltammetry techniques. Adherent and homogeneous PPy–P and PPy–W films were obtained. The corrosion behavior of mild steel with phosphate (PPy–P) and tungstenate (PPy–W) composite coatings in 3.5% NaCl solutions were investigated through a potentiodynamic polarization technique, open-circuit potential–time curves, and electrochemical impedance spectroscopy (EIS). On the basis of a physical model for corrosion of mild steel composites, Zview (II) software was applied to the EIS to estimate the parameters of the proposed equivalent circuit. It was found that the PPy–W coatings could provide much better protection than the PPy–P and polypyrrole coatings. The effects of the phosphate and tungstenate process parameters on the morphology and structure of the passive films were investigated by scanning electron microscopy and electron dispersion X-ray analyses. The results reveal that the PPy–P and PPy–W coated electrodes offered a noticeable enhancement in protection against corrosion processes. © 2008 Wiley Periodicals, Inc. J Appl Polym Sci 110: 2733–2741, 2008

Key words: coatings; composites; conducting polymers; electrochemistry; polypyrroles

INTRODUCTION

During previous decades, chromates have been widely used for the corrosion prevention of steel. Because chromium(VI) is, however, considered as carcinogen,[1] a considerable reduction of the amount of Cr(VI) from the previously permissible exposure limit has been required.[2] From an environmental view point, chromates should be replaced by a nontoxic substitute. Conductive polymers are thought to be one candidate for chromate replacement because their oxidative and catalytic properties induce a stable passive state in steels.[3–5] Conducting polymers, because of their nontoxicity, environmental friendliness, stability, and ease of synthesis, are one of the most promising coatings for the corrosion protection of metals.[1,2] During pyrrole (Py) electropolymerization, a positive charge is incorporated into the polypyrrole (PPy) matrix and is compensated for by anions doped from the electrolyte. The kind of counterions doped in the polymer matrix significantly affects the properties of the PPy film. There have been many reports concerning electrochemical synthesis of PPy films with various types of dopants, including organic[6–10] and inorganic ions.[11–13] Among organic anions, doped aliphatic and aromatic sulfonates provide good electrical and mechanical properties and good stability for the PPy layer.[14] Inorganic ions, such as ClO^-_4 or Cl^-, have also been doped in PPy; however, they were easily released during reduction, and other anions were incorporated from aqueous solution during the following oxidation.[15,16] The size of the counterions plays an important role in the exchange of doped anions.[17] When one selects large-size anions as the dopant, the anions are fixed in the PPy matrix, and cations are contrarily mobile as the charge compensation species. A PPy coating, to which molybdophosphate ions $PMo_{12}O^{3-}_{40}$, PMo_{12}, and naphthalene disulfonate anions were doped was prepared on steels to be applied to the corrosion prevention of steels.[18,19] The application of conducting polymers to the corrosion protection of metals is, however, subject to some limitations. First, a charge stored in the polymer layer can be irreversibly consumed during the system's redox reactions. Consequently, the protective properties of the polymer coatings may be lost with time. Also, the porosity and anion-exchange properties of the conducting polymers could be

Correspondence to: M. G. Hosseini (mg-hosseini@tabrizu.ac.ir).

disadvantageous, particularly when it comes to pitting corrosion caused by small aggressive anions (e.g., chloride anions). Interest has been focused on conducting-polymer-based composite coatings.[3] Recently, we systematically investigated the formation of polypyrrole and polyaniline with phosphate, tungstenate, and molybdate composites on mild steel from aqueous oxalate solutions.[20–22] The adhesion of the conductive polymer coating to the steel was dependent on the nature of the passivator (e.g., WO_4^{-2}, PO_4^{-3} and MoO_4^{-3}) and the passive interface formed on the steel before the electropolymerization of the polymers. Polyoxometalates are large metal cluster anions formed mainly by transition metals and oxygen atoms, which can adopt a variety of spatial structures. These can be incorporated as dopant anions into a conducting polymer matrix. Bonastre et al.[23] used a compact hybrid PPy–PWO^{-2}_4; their films were electrochemically synthesized on a carbon steel electrode in freshly prepared acetonitrile solutions. Their results show that the composite, PPy–PWO^{-3}_4, provided good protection against the corrosion of the polymer coatings on carbon steel in different solutions.

In this study, compact hybrid polypyrrole–phosphate (PPy–P) and polypyrrole–tungstenate (PPy–W) composite film were electrochemically synthesized on mild steel electrodes in aqueous solutions by the cyclic voltammetry (CV) method. The protective performance against corrosion of these coatings was evaluated with electrochemical impedance spectroscopy (EIS) in 3.5% NaCl solutions. The film morphology and composition were characterized by scanning electron microscopy (SEM) and energy-dispersive X-ray analysis.

EXPERIMENTAL

Py and oxalic acid were purchased from Merck Chemical Company, Inc., Darmstadt, Germany PPy was purified by distillation *in vacuo* and, just before use, stored at low temperature (0°C) in the dark. The aqueous solutions used in the experiments were prepared with deionized water. The samples used in this study were mild steel [MS; C (0.10 wt %), Mn (0.45 wt %) S (0.035 wt %), and P (0.06 wt %)] mounted in a Teflon holder, and the exposed electrode area was 0.25 cm^2. Before each experiment, the working electrode was polished with emery paper (1200 grit), rinsed with distilled water, and then electropolished at 4.0 V in a solution containing 50 g/L NaOH at 50°C; rinsed in distilled water and activated by immersion in 0.1*N* HCl for 3 s. The mild steel was rinsed twice before the electrochemical studies. The solution was deaerated with purified nitrogen for 20–30 min before the beginning of each experiment. The electropolymerization was performed in a one-compartment, three-electrode cell with Pt gauze as the counter electrode and a saturated calomel electrode (SCE) the reference electrode. An EG&G Princeton Applied Research 273A (TN) potentiostat/galvanostat was used as the power supply. The PPy film and PPy–P and PPy–W composites were obtained by electropolymerization from an aqueous solution of 0.1*M* Py + 0.1*M* oxalic acid and the same electrolyte with 0.001*M* sodium phosphate and 0.001*M* sodium tungstenate, respectively. We carried out CV by scanning from −0.6 to +1.2 V followed by reversing the scan to −0.6 V (SCE) for the first cycle. Then, the upper potential was restricted to +1 V for the next 10 cycles. Because the PPy coatings had overoxidation, the potential was higher than +1 V. The protective properties of the PPy, PPy–P, and PPy–W films were investigated in a 3.5% NaCl solution by Tafel polarization, open-circuit potential (OCP) and EIS measurements. Tafel polarization measurements were carried out on the protective corrosion of the PPy film and PPy–P and PPy–W composites in 3.5% NaCl at a sweep rate of 1 mV/s. Impedance measurements were carried out at the open-circuit potential (E_{ocp}) with a computer-controlled potentiostat (PAR EG&G model 273A and frequency response detector 1025). In the conventional three-electrode assembly, a Pt foil auxiliary electrode and a reference SCE were used. The alternating-current frequency range extended from 100 kHz to 10 mHz, with a 10-mV peak-to-peak sine wave being the excitation signal. The real and imaginary components of EIS in the complex plane and bode plots were analyzed with Zview (II) software (Scriber Assol., Inc.) to estimate the parameters of the equivalent electrical circuit. A scanning electron microscope (Philips XL30, Eindhoven, The Netherlands) was used to characterize the surface morphology and analysis of the polymer films.

RESULTS AND DISCUSSION

Electrochemical preparation and characterization of PPy and the PPy–W and PPy–P composites

Figure 1 shows the cyclic voltammograms obtained for mild steel electrodes in the same conditions mentioned previously. Figure 1 illustrates that, during Py electropolymerization, only a single peak appeared due to monomer oxidation (peak 1), and no significant electrochemical process occurred on the electrode in the studied region with phosphate and tungstenate anions, but the growth of PPy depended on the nature of the anions. Trivedi et al.[24] reported similar results during aniline electropolymerization. When the polymerization process is initiated, it is influenced by the anion for the following reasons: adsorption of the anion on the electrode surface, the redox potential of the anion, ionic

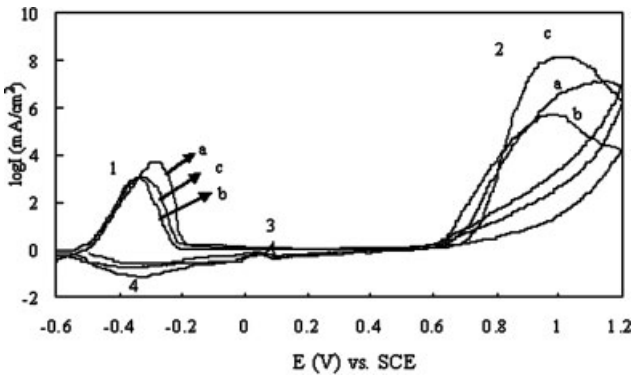

Figure 1 First cycle during (a) Py, (b) Py–phosphate, and (c) Py–tungstenate electropolymerization on the mild steel electrode (scan rate = 50 mV/s). E, potential; I, current.

charge, and ionic size. The peak potential values for the characteristic oxidation–passivation and repassivation processes for mild steel electrode were found to be −0.2 and +0.150 V, respectively. The synthesis of PPy and the PPy-based composite phosphate and tungstenate were carried out with the CV technique in two steps. First, a single cycle was taken in the potential range from −0.6 to +1.2 V versus SCE (Fig. 1) with a scan rate of 50 mV/s, and then 10 cycles were applied potential (<−0.6 vs 1 V) with the same scan rate. Satoh et al.[25] suggested that at lower applied potentials (<0.6 V vs SCE), the rate of polymerization is very slow, whereas at very high applied potentials (>1.0 V vs SCE), undesirable side reactions, such as ring opening and the breaking of conjugated bonds, may take place, which may result in the formation of defects and films with low conductivity. Figure 1 illustrates the electropolymerization of PPy, PPy–P, and PPy–W on mild steel electrodes. It is clearly evident that the active dissolution of mild steel started around −0.5 V (peak 1) and was followed by the passivation process. The maximum potential and current related to this peak decreased when tungstenate and phosphate anions existed in the electropolymerization solution. This may have been due to inhibition behavior of phosphate and especially tungstenate anions and better passivation of mild steel when these anions existed in the electropolymerization solution. Ahmad and MacDiarmid[26] attributed this influence on the protection time to the modification of the passive film, which was assumed to be the phosphate/oxide bilayer, whereas Macdiarmid et al.[26] believed that phosphoric acid reacts with iron and forms a $FeHPO_4$ layer to provide better adhesion and better protection. The dissolution process followed by the appearance of a passivity was around −0.2 V. For mild steel, electrode passivity of the surface was achieved before Py electropolymerization. Also, it seemed that the phosphate and tungstenate anions took part in the passivity process (peak 1). However, the electropolymerization process and its rate may have been affected by this composition change on the surface electrode. In the case of the mild steel electrode, the active dissolution of mild steel started around the potential value of −0.5 V (Fig. 1, peak 1), and then, there was a tendency to provide passivation of the surface. This intense dissolution of mild steel also prevented the formation of an adherent and homogeneous polymer film on the surface. This event was not observed on the platinum electrode (not shown here). The continuation of the positive scan rate (peak 2) appeared around 0.7 V, and the current sharply increased. This was due to monomer oxidation. In the reverse scan rate (cathodic branch, Fig. 1), two peaks were observed. One peak appeared around zero potential (peak 3), and the second peak was at −0.4 V (peak 4, Fig. 1). We suggest that the third peak (peak 3) may have been related to the passivation and repassivation of the surface. This peak in the electropolymerization of polyaniline[22] was strongly observed (not shown here) but was very weak in the electropolymerization of PPy. The weak repassivation peak indicated the formation of a more compact and adherent film. Peak 4 was strong, which was probably related to the reduction of PPy coating. During the reduction process, some phosphate and tungstenate anions pasted in the polymer were probably realized. Effectively, Beck et al.[27] and Mengoli and Musiani[28] already observed the same behavior in the case of an iron electrode polarization oxalic acid solution; the authors attributed this anodic wave to a new iron oxidation accompanied by the rebuilding of the FeC_2O_4 layer. By analogy, in our case, a similar process leading to the reconstruction of the $FeC_4H_4O_5$ layer on the working electrode surface could be assumed.

SEM and EDAX analysis

Figure 2 shows SEM micrographs of the PPy films and their composites on mild steel fabricated by the CV technique. As observed, the surface morphology of PPy changed in the presence of phosphate and tungstenate anion additives, as shown by the comparison of Figures 2(a), 2(b), and 2(c). It is illustrated that the pure PPy film exhibited a rougher surface morphology than the PPy–P and PPy–W composites. Also, a SEM micrograph for the PPy–P [Fig. 2(b)] and PPy–W [Fig. 2(c)] composites proved that the coating's structure was compact and the spatial distribution of phosphate and tungstenate particles in the composite was quite uniform. Line scan analysis confirmed the presence of phosphate [Fig. 3(a)] and tungstenate [Fig. 3(b)] compounds in the film compositions. During electropolymerization, some phosphate and tungstenate were incorporated into the polymer.

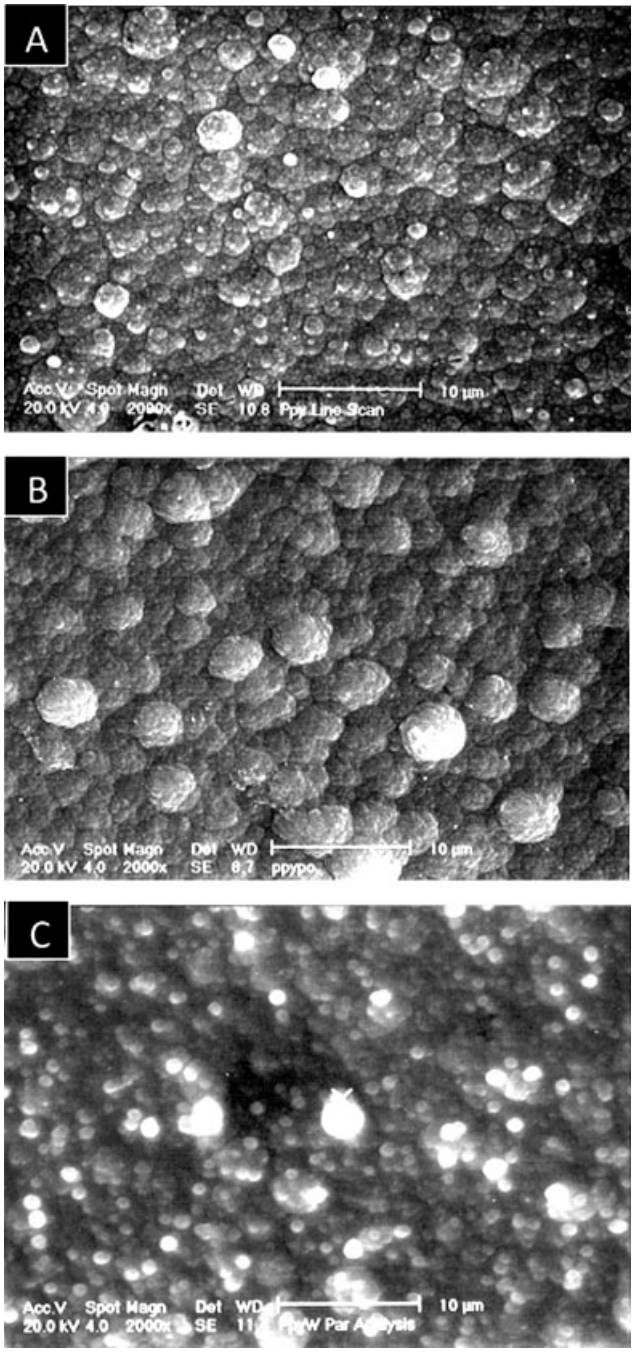

Figure 2 SEM micrograph obtained from the PPy films grown potentiodynamically in (a) 0.1*M* oxalic acid + 0.1*M* Py, (b) 0.1*M* oxalic acid + 0.1*M* Py + 0.001*M* sodium phosphate after the first CV scan between −0.6 and 1 V (SCE), and (c) 0.1*M* oxalic acid + 0.1*M* Py + 0.001*M* sodium tungstenate after the first CV scan between −0.6 an 1 V (SCE).

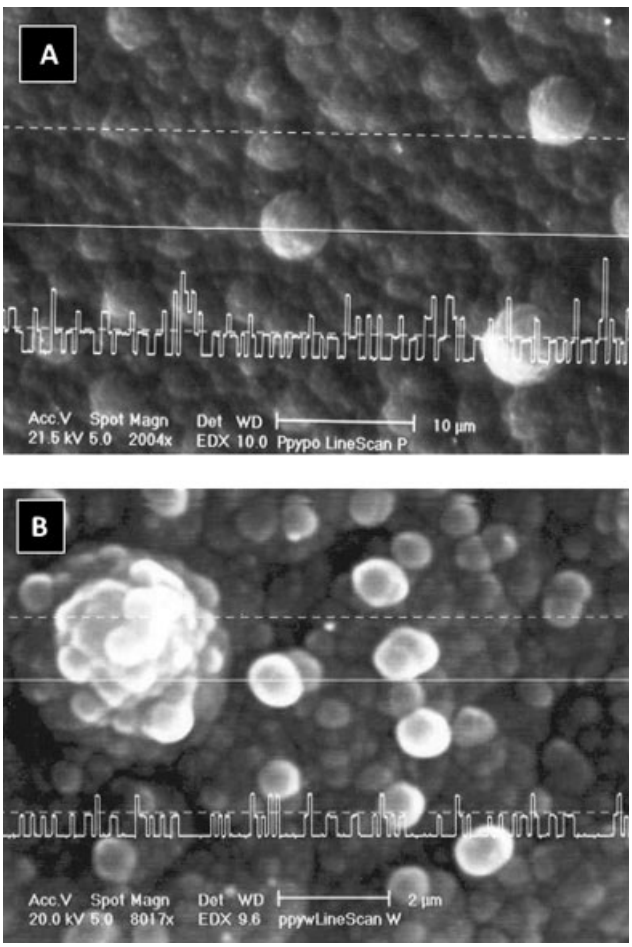

Figure 3 Energy-dispersive X-ray analysis of the composite coatings showing the existence of the phosphate and tungstenate components in the film layer. The SEM micrograph was obtained from PPy films with composites grown potentiodynamically under the same conditions as in Figure 4. The phosphorous line scan is also shown in Figure 4(b).

Evaluation of the corrosion performance

OCP monitoring and polarization technique

Figure 4 shows the evolution of OCP for PPy and the PPy–P and PPy–W composite films on mild steel in a corrosive solution (3.5% NaCl). The monitoring of OCP of the system allowed the assessment of the corrosion protection of mild steel by PPy and the PPy–P and PPy–W composites. Also, a more ennobling effect was observed in the presence of the

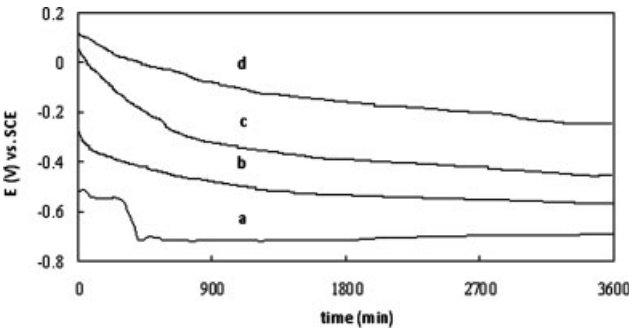

Figure 4 OCP monitoring for (a) bare mild steel, (b) mild steel/PPy, (c) mild steel/PPy–P, and (d) mild steel/PPy–W electrodes in a 3.5% NaCl solution after 1 h of immersion.

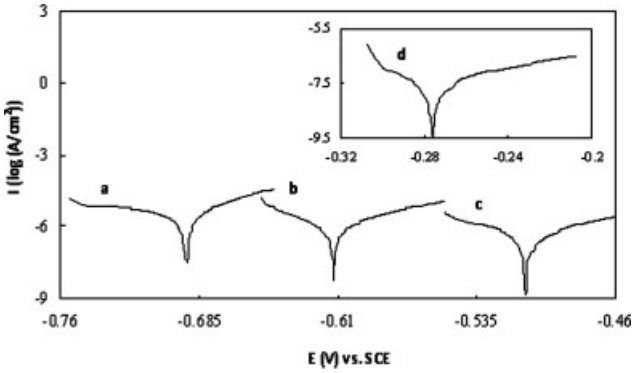

Figure 5 Tafel plots of (a) bare mild steel, (b) mild steel/PPy, (c) mild steel/PPy–P, and (d) mild steel/PPy–W electrodes in a 3.5% NaCl solution after 1 h of immersion (scan rate = 0.166 mV/s).

PPy–W and PPy–P composite films compared to the PPy film. For all of the studied PPy films, E_{ocp} at the beginning of the measurement showed a less negative potential, but the evolution was not the same for two films. With the pure PPy film, E_{ocp} decreased toward the corrosion potential (E_{corr}) of uncoated mild steel, and the metal was no longer protected. The coated steel initially exhibited potentials around 0.150, 0.06, and −0.270 V for PPy–W, PPy–P, and PPy, respectively. This relatively high potential indicated that the steel was passivated by the oxidative PPy layers, especially in the presence of anion passivators (tungstate and phosphate), whereas the potential of the bare steel was −0.64 V in the active dissolution region. The difference in potential at the initial stage between both coatings was high. During the time period at which the potential was maintained in the passive region, no appreciable corrosion took place. After 2 h of immersion, OCP was obtained as a pseudo-plateau. These values were −270 mV [Fig. 4(c), PPy–P], −120 mV [Fig. 4(d), PPy–W], and −470 mV [Fig. 4(b), PPy alone]. Fluctuations in the potential may have represented the anionic exchange of chloride and solvent exchange between the polymer film and the solution during equilibration in the 3.5% NaCl solution.[29]

Tafel polarization

As complementary experiments, Tafel polarization curves (Fig. 5) for different electrodes (bare mild steel, pure PPy, and the PPy–P and PPy–W composites) in the corrosive solution were plotted. Information on the corrosion rate and current density can be obtained by the Tafel extrapolation method. Table I illustrates the corrosion parameters for bare mild steel and mild steel coated with PPy, PPy–P, and PPy–W in 3.5% NaCl solutions. The iron(II) oxalate coated steel possessed a lower E_{corr} and a higher corrosion current (I_{corr}) than bare steel, which indicated that the iron(II) oxalate films were poor corrosion inhibitors for steel. However, it is clear from Table I that the PPy, PPy–P [Fig. 5(c)], and especially the PPy–W coatings significantly [Fig. 5(d)] increased E_{corr} and sharply reduced I_{corr}. The corrosion rates of the PPy–W and PPy–P coated steel significantly decreased as a result of the reduction in I_{corr}. These results indicate that PPy–W and PPy–P acted as a protective layer on the steel and improved the overall corrosion performance. The Tafel polarization curves showed that the PPy–W, PPy–P and PPy composite films caused a positive displacement in E_{corr} relative to the value of the bare mild steel electrode. Table I shows that the E_{corr} values were −697 for bare steel, −578 for PPy, −463 for PPy–P, and −267 for PPy–W. This positive displacement was higher for the PPy–W composite coating than for the PPy–P and PPy composite films. These shifts in E_{corr} confirmed the best protection of the metal surface when the composite was deposited. These measurements corroborated the qualitative results obtained previously with OCP and the potentiodynamic technique. The Tafel measurements clearly showed that a substantial reduction in the corrosion rate occurred for the coated sample with respect to the uncoated sample. This reduction may have been due to the inhibitory effect of phosphate anions. We suggest that phosphate and especially tungstenate anions may have diffused to the metal/polymer interface and were also released during the reduction of the polymer. However, in two states, phosphate anions can act as corrosion inhibitors to reduce the rate of corrosion. It was reported that

TABLE I
Tafel Polarization Parameters for the Corrosion of Mild Steel and PPy Composites in 3.5% NaCl

State	E_{corr} (mV; SCE)	I_{corr} (μA/cm^2)	$\beta_a \times 10^3$ (V/decade)	$\beta_c \times 10^3$ (V/decade)	Corrosion rate (mpy)
Bare mild steel	−697	23.9	44	87	44
MS/PPy	−578	19.2	24	28	35.4
MS/PPy–PO_4^{3-}	−463	4.16	67	69	7.67
MS/PPy–WO_4^{2-}	−267	0.241	14	33	0.445

β_a and β_c are anodic and cathodic Tafel slopes, respectively. MS, mild steel.

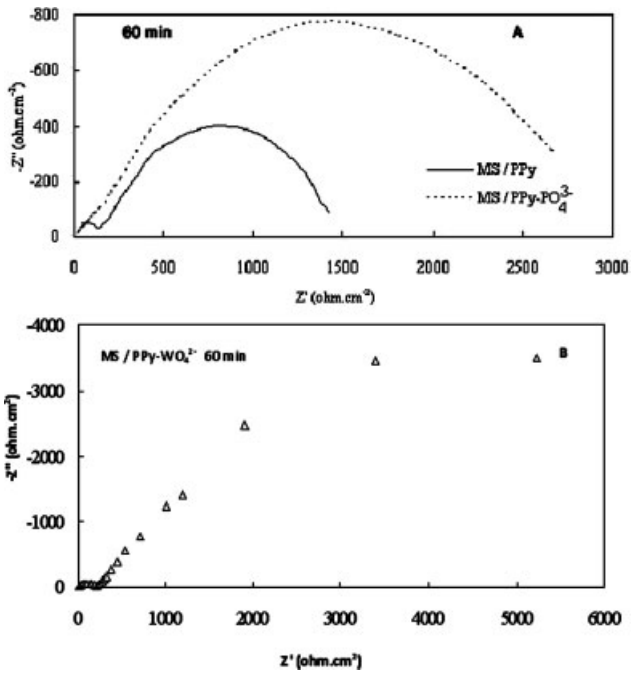

Figure 6 Nyquist plots for (A) Ms/PPy and Ms/PPy–P and (B) Ms/PPy–W electrodes in a 3.5% NaCl solution after 1 h of immersion. The fitted and experimental data are represented by solid lines and points, respectively.

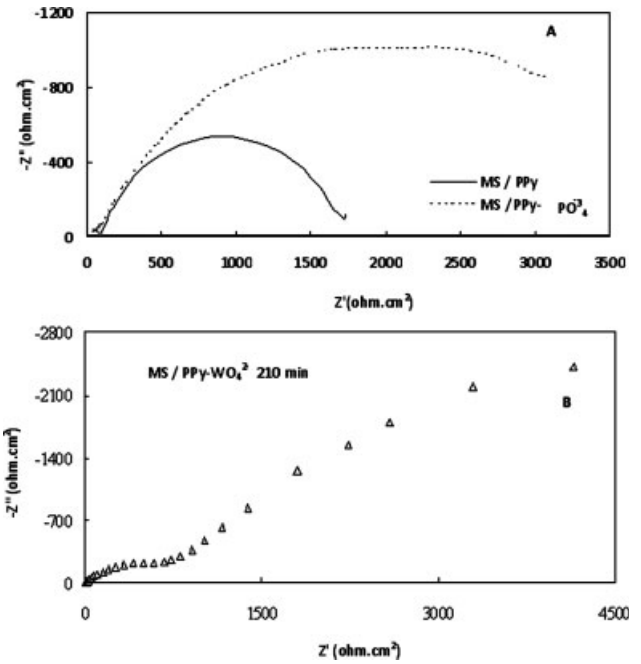

Figure 7 Nyquist plots for (A) Ms/PPy and Ms/PPy–P and (B) Ms/PPy–W electrodes in a 3.5% NaCl solution after 210 min of immersion. The fitted and experimental data are represented by solid lines and points, respectively.

PPy coatings have auto-undoping properties during immersion in corrosive solutions,[26,30,31] which is in agreement with our suggestion.

EIS

EIS is a measurement technique that allows for a wide variety of coating evaluations. The corrosion performance of the PPy, PPy–W, and PPy–P coatings deposited on steel were investigated by EIS. EIS measurements confirmed the potentiodynamic and OCP results. EIS data was recorded after various exposure times in 3.5% NaCl solutions. Nyquist plots were constructed and an appropriate equivalent circuit model was used to correlate the impedance with the capacitance and the resistance of the films. Figures 6 and 7 show examples of Nyquist plots for PPy–P [Figs. 6(A) and 7(A)] and PPy–W [Figs. 6(B) and 7(B)] after 60 and 210 min of immersion, respectively. Equivalent circuit models for these substrates are illustrated in Figure 8, and the values are given in Table II. Figure 8 shows the proposed equivalent circuit for mild steel/PPy and PPy–W for immersion times of 0–180 min [Fig. 8(a)], PPy–W for immersion times of 0–180 min [Fig. 8(b)], and mild steel/PPy–P electrodes [Fig. 8(c)]. This circuit for the PPy–P composite coatings is a two-time constant circuit in series. Figure 9 shows an example comparison between the experimental and simulated data for PPy and PPy–W after 120 min of exposure in 3.5% NaCl solutions. There was a good fit to the experimental data. Fitting analysis was applied to the impedance spectra in Figure 7 to estimate the elements of the equivalent circuit given in Figure 8. Fitted curves are represented by solid lines, and the experimental data are represented by circuit points. The given equivalent circuit provided a good fit to the experimental data. Two depressed semicircles at the high and low frequencies were assigned to reactions at the polymer/electrolyte and metal/polymer interfaces, respectively. The first partially seen semicircle

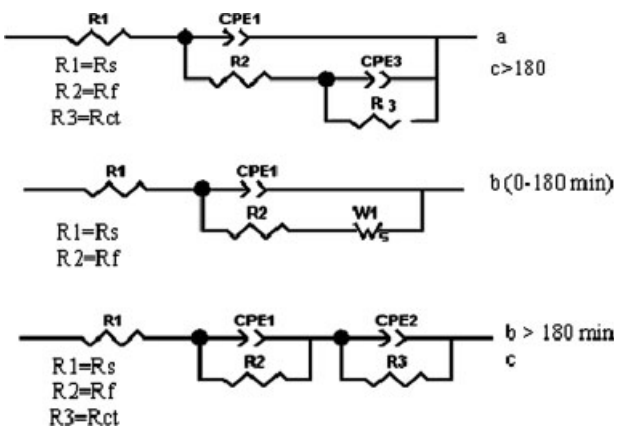

Figure 8 Proposed equivalent circuit for (a) mild steel/PPy, (b) mild steel/PPy–W (time immersion = 0–180 min, and (c) mild steel/PPy–P electrodes.

TABLE II
Impedance Data Obtained by the Simulation of EIS Measurement Related to Mild Steel

						Warburg (Ws)		
State	Time (min)	R_s (Ω cm^2)	R_{ct} (Ω cm^2)	$Y_0 \times 10^5$ (Ω^{-1} cm^{-2})	n1	Ws-R (Ω cm^2)	Ws-T (Ω^{-1} cm^{-2})	Ws-P
MS	120	0.425	50.1	93.2	0.93	512	2.8	0.40

R_s, the solution uncompensated resistance between working and reference electrodes; MS, mild steel; Y_o, constant phase element admittance; $n1$, constant phase element exponent; *W*s, warburg impendance element; *W*s-R, warburg impendence element resistance; *W*s-T, warburg impendence element admittance; *W*s-P, warburg impendence element exponent.

at the high-frequency region was related to polymer film resistance (R_f). The second one at the middle- and low-frequency region was attributed to charge-transfer resistance (R_{ct}) for processes occurring at the bottom of the pores of the coatings.[31,32]

Figure 10 shows a comparison between experimental and simulated data for PPy–W after 210 min of exposure in a 3.5% NaCl solution. After a higher immersion time of 180 min [Fig. 8(b), proposed equivalent circuit], the behavior of PPy–W was different from times lower than 180 min [Fig. 8(a), proposed equivalent circuit]. The calculated EIS parameters for mild steel, and mild steel/PPy, mild steel/PPy–P, mild steel/PPy-W composite coatings are presented in Tables II and III, respectively. The R_{ct} values obtained for the PPy–W (1532.5 Ω cm^2) and PPy–P (951.25 Ω cm^2) electrodes were relatively high with respect to those observed for PPy (367.50 Ω cm^2) and uncoated mild steel (50.1 Ω cm^2) at 210 min of immersion. This increase was related to the decrease in the charge-transfer rate between the metal and the solution. Charge-transfer reactions are known to take place at metal/polymer interfaces. Consequently, the high R_{ct} values of the PPy–W and PPy–P electrodes can be explained by the effective

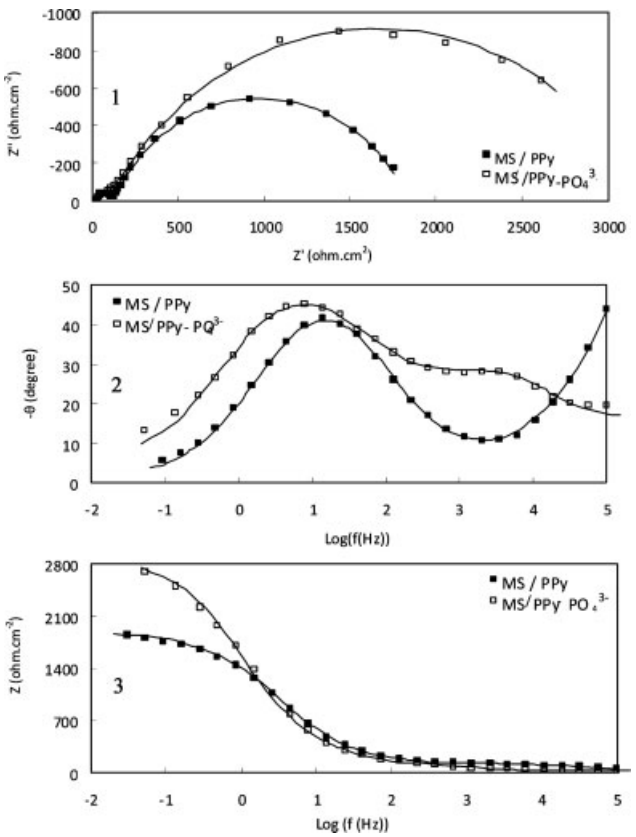

Figure 9 (1) Nyquist plot, (2) bode plot (angle), and (3) bode plot (modulus) of mild steel/PPy and mild steel/PPy–P electrodes in a 3.5% NaCl solution after 120 min of immersion time. The fitted and experimental data are represented by solid lines and points, respectively.

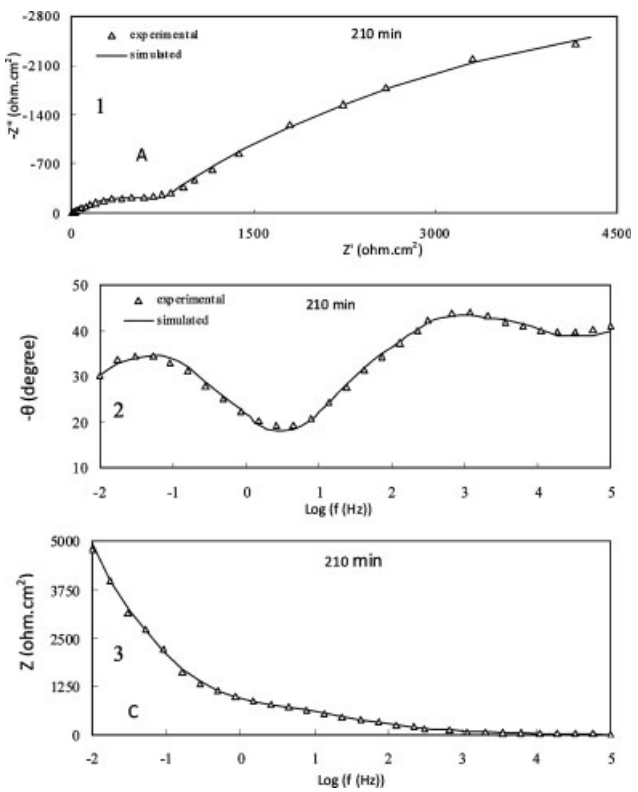

Figure 10 (1) Nyquist plot, 2) bodes plot (angle), and (3) bode plot (modulus) of mild steel/PPy–W electrodes in a 3.5% NaCl solution after 210 min of immersion time. The fitted and experimental data are represented by solid lines and points, respectively.

TABLE III
Impedance Data Obtained by the Simulation of EIS Measurement Related to Mild Steel Coated by PPy, PPy–P, and PPy–Tungstenate Coatings

TATE	Time (min)	R_s (Ω cm^2)	R_{ct} (Ω cm^2)	$T_{metal} \times 10^5$ (Ω^{-1} cm^{-2})	P (metal)	R_f (Ω cm^2)	$T_{coat} \times 10^5$ (Ω^{-1} cm^{-2})	P (coat)
MS/PPy	30	5.84	122.50	34.01	0.59	81.66	3.76	0.43
	60	4.86	266.75	41.20	0.69	53.90	2.40	0.50
	90	4.75	350	34.02	0.72	47.75	2.47	0.51
	120	4.59	377.50	32.80	0.73	45.41	1.73	0.52
	150	4.39	372	34.80	0.73	37.61	1.19	0.55
	180	3.91	358.25	32.40	0.74	44.08	1.86	0.48
	210	3.63	367.50	31.20	0.75	37.62	1.01	0.55
	240	3.44	369.75	30.40	0.75	33.10	0.82	0.57
MS/PPy–PO_4^{3-}	30	5.25	733.75	20.84	0.73	22.62	23.50	0.59
	60	5.00	626.25	38.44	0.67	31.25	29.02	0.58
	90	5.00	738.75	45.56	0.67	31.25	35.95	0.56
	120	4.50	754.75	53.60	0.68	18.25	36	0.56
	150	4.50	985	54.00	0.66	14.06	37.35	0.53
	180	4.75	916.75	57.20	0.67	11.00	40.88	0.53
	210	4.75	951.25	40.00	0.70	19.00	33.6	0.548
	240	5.00	996.25	37.20	0.70	11.75	37.20	0.52

						Warburg (Ws)		
MS/PPy–WO_4^{2-}	Time (min)	R_s (Ω cm^2)	R_f (Ω cm^2)	$T_{coat} \times 10^5$ (Ω^{-1} cm^{-2})	P (coat)	Ws-R (Ω cm^2)	Ws-T (Ω^{-1} cm^{-2})	Ws-P
	30	2.23	47	2.8	0.62	2682	38.79	0.72
	60	2.40	48	1.6	0.67	3176	148	0.68
	90	2.57	55	2.35	0.66	3075	152	0.71
	120	3.22	60	6.61	0.59	3051	164	0.71
	150	4.65	86	28.6	0.50	3027	164	0.73
	Time (min)	R_s (Ω cm^2)	R_{ct} (Ω cm^2)	$T_{metal} \times 10^5$ (Ω^{-1} cm^{-2})	P (metal)	R_f (Ω cm^2)	$T_{coat} \times 10^5$ (Ω^{-1} cm^{-2})	P (coat)
	180	5.53	3210	441	0.70	122.9	33.66	0.53
	210	5.39	1532.5	439.60	0.69	187.11	35.34	0.55
	240	5.22	662.5	349.03	0.75	419.78	29.20	0.56

R_s, the solution uncompensated resistance between working and reference electrodes; T_{metal}, metal corrosion conductance (reciprocal of R_{metal}); P, constant phase element exponent; T_{coat}, coating conductance (reciprocal of R_{coat}); *W*s, Warburg impendence element; *W*s-R, warburg impendence element resistance; *W*s-T, Warburg impendence element admittance; *W*s-P, Warburg impendence element exponent.

barrier behavior of the polymer films. Also, the maintenance of the passive layer formed before the electropolymerization process started may have had an effect on this increase.[33] Comparison between the PPy and PPy–P coatings indicated that the charge-transfer values were higher for the PPy–P coating. Barrier properties of the coating decreased after 240 min of immersion. This was because of the uptake of water and Cl^- into the coating. We believe that the decrease in total impedance after 60 min of immersion may have been due to the diffusion of Cl^- anions to the metal/polymer interface and their buildup in this place. So increase in the total impedance after this period of time may be related to the buildup of these anions in this place and their inhibitory effect. The values of the circuit parameters are addressed in Table III. We concluded that the phosphate anions could not have prevented the uptake of water. However, the uptake of chlorine species may have been restricted because of the polyvalent nature of the phosphate anions. We believe that

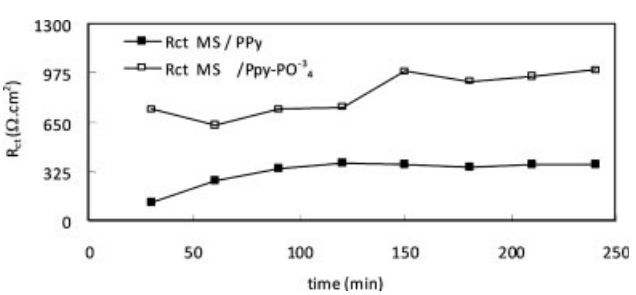

Figure 11 R_{ct} change versus time of PPy and PPy–P electrodes in a 3.5% NaCl solution.

polymeric films in this state bore negatively charged species and thus were capable of blocking the access of pitting-causing anions to the surface of mild steel. EIS measurements confirmed the potentiodynamic and OCP results. On the basis of these EIS results, we concluded that the immersion time had a significant effect on the impedance of the samples. Moreover, Figure 11 demonstrates R_{ct} versus time of the PPy and PPy–P electrodes in 3.5% NaCl solutions. We observed that the change in R_{ct} and the coating resistance change values for the PPy–P and PPy–W composites were higher than that of PPy alone.

CONCLUSIONS

In the first part of this article, the electrosynthesis of PPy and PPy–P and PPy–W composites on mild steel by CV in oxalic acid medium were discussed. The results revealed that the polymerization process was influenced by the anion on the electrode surface, the redox potential of the anion, the ionic charge, and the ionic size. Furthermore, the SEM results illustrate that PPy exhibited a rougher surface morphology than the PPy–W and PPy–P films. The PPy layers were porous, and the protection depended on the quality of the oxide film. In the second part of the article, the corrosion behavior of mild steel that was covered by the electrodeposited PPy–W, PPy–P, and PPy films in corrosive 3.5% NaCl media was discussed. Of the all layers, the PPy–W layer proved to offer better protection; that is, OCP was established in the passive region for a longer period of time under the given experimental conditions. The anodic polarization study clearly showed that a shift in the potential in the PPy–P and especially the PPy–W composite related to PPy. The Tafel polarization measurements showed that the corrosion protection of the PPy–W composite was higher than those of the PPy–P and pure PPy. The results of EIS confirmed the results of the polarization methods. The charge-transfer values and the total impedance for the PPy–W composite were higher than those of PPy–P and pure PPy. From the EIS results, we concluded that, after the diffusion of tungstenate and phosphate anions to the metal/polymer interface and the buildup of them in this phase, they acted as inhibitors on the surface. A comparison of the impedance results also showed an enhancement in the protective performance of PPy–P and PPy–W with respect to PPy alone. Moreover, with regard to the EIS studies, the participation of tungstate and phosphate dopants in the passivation process and, consequently, the formation of PPy–W and PPy–P, resulted in a primary passive layer with higher quality. In fact, the formation of this layer under the PPy–coating increased the corrosion protection ability of this new PPy coating for mild steel. This process may be useful in the formation of undercoats for paints and polymer coatings on mild steel.

The authors thank the Electrochemistry Research Laboratory of Tabriz and Tarbiat Modarres Universities.

References

1. Kretchik, J. T. J Chem Health Saf 2006, 13, 39.
2. Fed Regist 2006, 39, 10103.
3. Wessling, B. Adv Mater 1994, 6, 226.
4. Lu, W. K.; Elsenbaumer, R. L.; Wessling, B. Synth Met 1995, 71, 2163.
5. Tuken, T.; Yazici, B.; Erbil, M. Prog Org Coat 2004, 50, 115.
6. Suematsu, S. Y. O.; Tsujimoto, H.; Kanno, H. Electrochim Acta 2000, 45, 3813.
7. Cheah, K.; Forsyth, M.; Truong, V. T. Synth Met 1998, 94, 215.
8. Bazzaoui, M.; Martins, L.; Bazzaoui, E. A.; Martins, J. I. Electrochim Acta 2002, 47, 2953.
9. Bazzaoui, M.; Martins, J. I.; Reis, T. C.; Bazzaoui, E. A.; Nunes, M. C.; Martinis, L. Thin Solid Films 2005, 485, 155.
10. Nguyen, H.; Garcia, B.; Deslouis, C.; Xuan, Q. L. Electrochim Acta 2001, 46, 4259.
11. Hammache, H.; Makhloufi, L.; Saidani, B. Corros Sci 2003, 45, 2031.
12. Cho, K.; Chung, S. D.; Ryu, K.; Kim, Y.; Choy, J.; Kim, H. Synth Met 1995, 69, 481.
13. Bergamaski, F. O. F.; Santos, M. C.; Nascente, P. A. P.; Bulhoes, L. O. S.; Pereira, E. C. J Electroanal Chem 2005, 583, 162.
14. Bhattacharya, A.; Das, A. De S. Polymer 1996, 37, 4375.
15. Tüken, T. Prog Org Coat 2006, 55, 60.
16. Ohtsuka, T.; Iida, M.; Ueda, M. J. Solid State Electrochem 2006, 10, 714.
17. Martins dos Santos, L. M.; Lacroix, J. C.; Chane-Ching, K. I.; Adenier, A.; Abrantesa, L. M.; Lacaze, P. C. J Electrochem Soc 2006, 587, 67.
18. Tüken, T.; Özyılmaz, A. T;. Yazıcı, B.; Kardaş, G.; Erbil, M. Prog Org Coat 2004, 51, 27.
19. Kowalski, D.; Ueda, M.; Ohtsuka, T. Corros Sci 2007, 49, 1635.
20. Hosseini, M. G.; Shahrabi, T.; Sabouri, M. Mater Corros 2006, 57, 407.
21. Hosseini, M. G.; Seyedsajjadi, S. A.; Banazadeh, R.; Sharabi, T. Presented at the Eurocorr 2006 conference, 24 Sep 2006, Masstrghight, The Netherlands.
22. Hosseini, M. G.; Shahrabi, T.; Sabouri, M. Presented at the Eurocorr 2005 conference, 24 Sep 2005, Lisbon, Portugal.
23. Bonastre, J. A.; Huerta, F.; Quijada, C.; Vázquez, J. L.; Garcés, P.; Cases, F. Presented at the 15th International Corrosion Congress: Frontiers in Corrosion Science and Technology, 22–27 Sept 2002, Granada, Spain.
24. Trivedi, D. C. Solid State Electrochem 1998, 2, 85.
25. Satoh, M.; Kaneto, K.; Yoshino, K. J Appl Phys 1985, 24, 423.
26. Ahmad, N.; MacDiarmid, A. G. Synth Met 1996, 78, 103.
27. Beck, F.; Michaelis, R.; Schloten, F.; Zinger, B. J Electrochim Acta 1994, 39, 229.
28. Mengoli, G.; Musiani, M. M. Electrochim Acta 1986, 31, 201.
29. Ocón, P.; Cristobal, A. B.; Herrasti, P.; Fatas, E. Corros Sci 2005, 47, 649.
30. Bernard, M. C.; Joiret, S.; Hugot-Le Goff, A.; Long, P. D. J Electrochem Soc 2001, 148, B299.
31. Walter, G. W. Corros Sci 1986, 26, 681.
32. Moraes, R. S.; Huerta-Vilca, D.; Motheo, A. R. J. Eur Polym J 2004, 40, 2033.
33. Inzelt, G.; Pineri, M.; Schultze, J. W.; Vorotynetsev, M. A. Electrochim Acta 2000, 45, 2403.